

# Dust formation in very massive primordial supernovae

R. Schneider,<sup>1,2\*</sup> A. Ferrara<sup>3</sup> and R. Salvaterra<sup>3</sup>

<sup>1</sup>INAF/Osservatorio Astrofisico di Arcetri, Largo E. Fermi 5, 50125 Firenze, Italy

<sup>2</sup>Centro ‘Enrico Fermi’, Via Panisperna 89/A, 00184 Roma, Italy

<sup>3</sup>SISSA/International School for Advanced Studies, Via Beirut 4, 34100 Trieste, Italy

Accepted 2004 March 23. Received 2004 March 23; in original form 2003 July 4

## ABSTRACT

At redshift  $z \gtrsim 5$ , Type II supernovae (SNeII) are the only known dust sources with evolutionary time-scales shorter than the Hubble time. We extend the model of dust formation in the ejecta of SNeII by Todini & Ferrara to investigate the same process in pair-instability supernovae (PISNe), which are thought to arise from the explosion of the first, metal-free, very massive (140–260  $M_{\odot}$ ) cosmic stars.

We find that 15–30 per cent of the PISN progenitor mass is converted into dust, a value  $> 10$  times higher than for SNeII; PISN dust depletion factors (the fraction of produced metals locked into dust grains) range between 0.3 and 0.7. These conclusions depend very weakly on the mass of the PISN stellar progenitor, which in contrast affects considerably the composition and size distribution. For the assumed temperature evolution, grain condensation starts 150–200 d after the explosion; the dominant compounds for all progenitor masses are  $\text{SiO}_2$  and  $\text{Mg}_2\text{SiO}_4$  while the contribution of amorphous carbon and magnetite grains grows with progenitor mass; typical grain sizes range between  $10^{-3}$  and a few times  $0.1 \mu\text{m}$  and are always smaller than  $1 \mu\text{m}$ . We give a brief discussion of the implications of dust formation for the initial mass function evolution of the first stars, cosmic reionization and the intergalactic medium.

**Key words:** supernovae: general – dust, extinction – galaxies: formation – cosmology: theory.

## 1 INTRODUCTION

In recent years, dust has been recognized to have an increasingly important role in our understanding of the near and distant Universe. The dramatic effect of dust at low and moderate redshifts was immediately recognized when a reconstruction of the cosmic star formation history from rest-frame ultraviolet (UV)/visible emission was first attempted: dust grains absorb stellar light and re-emit it in the far-infrared (FIR). Thus even a tiny amount of dust extinction can lead to a severe underestimate of the actual star formation rate (Pettini et al. 1998; Steidel et al. 1999). New infrared (IR), FIR and submillimetre facilities have revealed the existence of populations of sources, such as SCUBA  $z \gtrsim 1$  sources, that are thought to be dust-enshrouded star-forming galaxies or active galactic nuclei (AGNs) (Smail, Ivison & Blain 1997; Hughes et al. 1998), or the ‘extremely red objects’, which are at least partly populated by dusty star-forming systems at  $z \sim 1$  (Cimatti et al. 2002). Finally, dust plays a critical role in galaxy evolution, accelerating the formation of molecular hydrogen ( $\text{H}_2$ ), dominating the heating of gas through emission of photoelectrons in regions where UV fields are present, and contributing to gas cooling through IR emission [see Draine 2003 for a recent thorough review].

This observational evidence has motivated a series of studies aimed at including a treatment of dust formation within galaxy evolution models (Granato et al. 2000; Hirashita & Ferrara 2002; Morgan & Edmunds 2003). Since dust formation in the interstellar medium (ISM) is extremely inefficient (Tielens 1998), the preferred sites of formation are considered to be the atmospheres of evolved low-mass ( $M < 8 M_{\odot}$ ) stars, from where it is transported into the ISM through stellar winds (Whittet 1992). However, this mechanism cannot explain the presence of dust at redshifts  $> 5$  because at these high redshifts the evolutionary time-scales of low-mass stars (0.1–1 Gyr) start to be comparable to the age of the Universe.

Evidence for the presence of dust at high redshifts comes from observations of damped  $\text{Ly}\alpha$  systems (Pettini et al. 1994; Prochaska & Wolfe 2002; Ledoux, Bergeron & Petitjean 2002) and from the detection of dust thermal emission from high-redshift QSOs selected from the Sloan Digital Sky Survey (SDSS) out to redshift 5.5 and re-observed at millimetre wavelengths (Omont et al. 2001; Carilli et al. 2001; Bertoldi & Cox 2002). Very recently, Bertoldi et al. (2003) have reported observations of three  $z > 6$  SDSS QSOs at 1.2 mm, detecting thermal dust radiation. From the IR luminosities, the estimated dust masses are huge ( $> 10^8 M_{\odot}$ ), implying a high abundance of heavy elements and dust at redshifts as high as 6.4 that cannot be accounted for by low-mass stars. Thus dust enrichment must have occurred primarily on considerably shorter time-scales in the ejecta of supernova (SN) explosions (Dwek & Scalzo 1980;

\*E-mail: raffa@arcetri.astro.it

Kozasa, Hasegawa & Nomoto 1989; Todini & Ferrara 2001; Nozawa et al. 2003).

The strongest evidence for dust formation in SN explosions was seen in SN 1987A (Moseley et al. 1989; Wooden 1997). In this event, the increased IR emission was accompanied by a corresponding decrease in the optical emission and the emission-line profiles were observed to shift toward the blue (McCray 1993, and references therein). In another SN explosion, SN 1998S, the observed evolution of the hydrogen and helium line profiles argues in favour of dust formation within the ejecta as the redshifted side of the profile steadily faded while the blueshifted side remained constant (Gerardy et al. 2000). Dust emission has been seen in the SN remnant Cassiopeia A: similarly to SN 1987A, the total dust mass derived from IR luminosities is less than expected from theory, suggesting that a colder population of dust grains may be present that emit at longer wavelengths and are not detectable in the IR (Morgan & Edmunds 2003; Dunne et al. 2003). Finally, in a considerable number of cases, SNe have shown IR emission that is stronger toward longer wavelengths [see Gerardy et al. (2002) and references therein]. This IR excess has been generally interpreted as due to thermal emission from dust forming in the ejecta, but alternative explanations exist: in particular, new IR observations of five Type II SNe (SNeII) have shown late-time emission that remains bright many years after the maximum and is hard to reconcile with emission from newly formed dust; IR echoes from pre-existing dust in the circumstellar medium heated by the SN flash might represent an alternative interpretation (Gerardy et al. 2002).

Theoretical studies have started to investigate the process of dust formation in expanding SN ejecta. Most of the available models are based on classical nucleation theory and grain growth (Kozasa & Hasegawa 1987; Todini & Ferrara 2001), with the exception of the computations recently performed by Nozawa et al. (2003), who have made an extensive analysis of the properties of dust grains forming in zero-metallicity SNe of various masses. The model developed by Todini & Ferrara (2001) is able to predict the dust mass and properties as a function of the initial stellar progenitor mass and metallicity. In spite of the many uncertainties and approximations, this model has been shown to reproduce satisfactorily the observed properties of SN 1987A and of the young dwarf galaxy SBS 0335-052 (Hirashita, Hunt & Ferrara 2002).

In this paper, we investigate the formation of dust grains in the ejecta of very massive primordial SNe, which are commonly known as pair-creation or pair-instability SNe (PISNe). These violent explosions are thought to terminate the life of metal-free stars with initial mass in the range  $140 \leq M \leq 260 M_{\odot}$  (Heger & Woosley 2002). Indeed, detailed theoretical modelling of the nucleosynthesis and internal structure of these very massive stars has shown that, after central helium burning, electron/positron pairs are created, converting a large fraction of internal energy into rest mass of the pairs; as a consequence, the stars rapidly contract until explosive oxygen and silicon burning is able to reverse the collapse and the stars are completely disrupted in giant explosions (Fryer, Woosley & Heger 2001). Below and above the mass range of PISNe, the most likely outcome of the evolution of metal-free stars appears to be black hole formation, cleanly separating the contribution to metal and eventually dust production of such very massive stars from that of other mass ranges.

We base our analysis on the model developed by Todini & Ferrara (2001) and apply it to PISNe. We therefore change the initial chemical composition of the ejecta and also the thermodynamical/dynamical properties which determine the ejecta evolution. A larger amount of dust is expected to form in the ejecta of PISNe with

respect to SNeII, because of the larger amount of metals released and the absence of fallback of material on to the compact remnant (no remnant is expected to survive PISN explosions).

The motivation for the present study comes from the increasing amount of evidence which seems to indicate that the first stars that were able to form in the early Universe from the collapse of metal-free gas clouds were indeed very massive, with characteristic masses of a few hundred  $M_{\odot}$ . This evidence includes detailed numerical simulations (Bromm, Coppi & Larson 1999, 2002; Abel, Bryan & Norman 2000, 2002; Bromm et al. 2001; Ripamonti et al. 2002), semi-analytic models (Omukai & Nishi 1998; Nakamura & Umemura 2001, 2002; Schneider et al. 2002) and several observations (Hernandez & Ferrara 2001; Oh et al. 2001; Salvaterra & Ferrara 2003). In particular, some of these studies have pointed out that, because of the reduced gas cooling efficiency, low-mass star formation is strongly inhibited before a minimum level of metal enrichment of the collapsing gas cloud has been reached (Bromm et al. 2001; Schneider et al. 2002). The value of this minimum level,  $Z_{\text{cr}}$ , is very uncertain, but likely to be between  $10^{-6}$  and  $10^{-4} Z_{\odot}$  (Schneider et al. 2002, 2004). Within this critical range of metallicities, the presence of dust appears to have a major role, providing an additional pathway for cooling the gas, which fragments into lower mass clumps, enabling the formation of second-generation low-mass stars (Schneider et al. 2003). Thus, to estimate the efficiency of this dust-regulated low-mass star formation channel in very metal-poor gas clouds, it is crucial to develop a model that is able to predict the amount of dust formed in the ejecta of PISNe.

## 2 DUST FORMATION MODEL

The process of dust formation and the resulting dust grain properties depend on the physical conditions at the site of formation. In particular, several studies [see Kozasa et al. (1989) and references therein] have shown that the time of onset of grain formation depends on the temperature structure in the SN ejecta, whereas the grain composition mainly reflects its chemical composition, which depends on the nucleosynthesis occurring during stellar lifetime (i.e. depends on the progenitor mass) and explosion.

Thus models of dust formation in SN ejecta are based on specific prescriptions for the chemical composition and thermodynamics of the expanding gas. At the onset of shock generation, which occurs at the boundary of the innermost Fe–Ni core, the progenitor star is characterized by the standard stratified (onion-skin) structure. During shock propagation through the star, the gas undergoes a new phase of (explosive) nucleosynthesis and mixing of the internal layers is thought to occur at least up to the outer edge of the helium layer, as suggested by observations of the early emergence of  $\gamma$ - and X-rays in SN 1987A [Kumagai et al. (1988) and references therein]. These observations confirm that macroscopic mixing of the ejecta occurs through Rayleigh–Taylor instabilities, but it is still debated whether mixing is extended to the molecular level (Clayton, Liu & Dalgarno 1999; Clayton, Deneault & Meyer 2001).

The model of Todini & Ferrara (2001) (but see also Kozasa et al. 1989) is based on the assumption that materials are uniformly mixed from the centre to the helium outer edge. As a consequence, the temperature and density within this metal-rich volume are assumed to be constant. When the shock reaches the surface of the progenitor, the star starts to expand and the expansion becomes homologous. Thus the velocity of gas at a given layer is constant in time and proportional to the radius from the centre, i.e.  $v = R/t$ , where  $t$  is the time from the explosion and the expansion velocity is assumed

to be

$$v = \left( \frac{E_{\text{kin}}}{M_{\text{tot}}} \right)^{1/2}, \quad (1)$$

where  $E_{\text{kin}}$  and  $M_{\text{tot}}$  are the kinetic energy and total mass ejected by the SN. The temperature of the expanding ejecta is determined by various heating and cooling mechanisms. Todini & Ferrara (2001), following Kozasa et al. (1989), assumed that when the gas reaches the photosphere, the gas temperature is equal to the photospheric temperature and thereafter the temperature evolution follows from the assumptions of adiabatic expansion for a perfect gas, so that

$$T = T_i \left( 1 + \frac{v}{R_i} t \right)^{3(1-\gamma)}, \quad (2)$$

where  $\gamma$  is the adiabatic index and the quantities  $T_i$  and  $R_i$  are the photospheric temperature and radius obtained from the observational results of SN 1987A (Catchpole et al. 1987). The lack of observational constraints for PISNe forces us to model the thermal evolution of the expanding ejecta on the basis of theoretical considerations. In particular, the evolution and internal structure of PISNe have been studied in great detail through numerical simulations (Fryer et al. 2001; Heger & Woosley 2002). Zero-metallicity progenitor stars with masses between 140 and 260  $M_{\odot}$  evolve without significant mass loss until central helium burning. These stars, after central helium depletion, have enough central entropy that they enter a temperature and density regime in which electron/positron pairs are created in abundance, converting internal gas energy into rest mass of the pairs, without contributing much to the pressure. When this instability is encountered, the stars contract rapidly until explosive oxygen and silicon burning produce enough energy to reverse the collapse and the stars are completely disrupted in a giant explosion. The maximum central temperature and density during the bounce as a function of the PISN progenitor mass, together with the elemental composition of the emerging ejecta, are shown in Fig. 1. The dominant metal yields show that nucleosynthesis in PISNe produces a total mass of O, Si, Mg and Al which is roughly independent

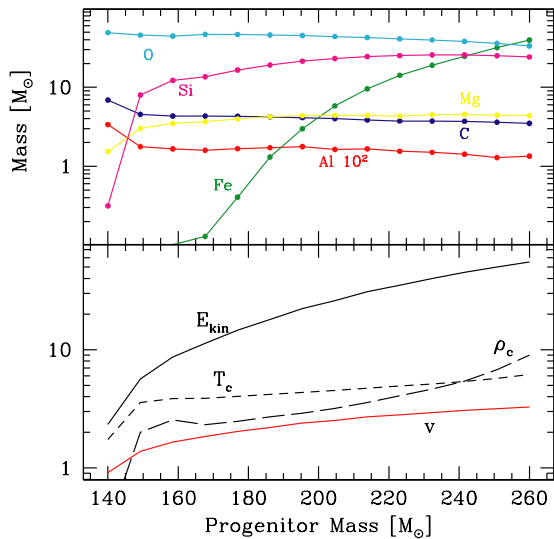


**Figure 1.** Top panel: dominant metal yields ( $M_{\odot}$ ) of a PISN (Heger & Woosley 2002) as a function of the progenitor stellar mass, after all unstable isotopes have decayed. Bottom panel: kinetic energy (in units of  $10^{51}$  erg), velocity of the ejecta (in units of  $10^3$  km  $s^{-1}$ ), central temperature (in units of  $10^9$  K) and density (in units of  $10^6$  g  $cm^{-3}$ ) as a function of the progenitor stellar mass (see text).

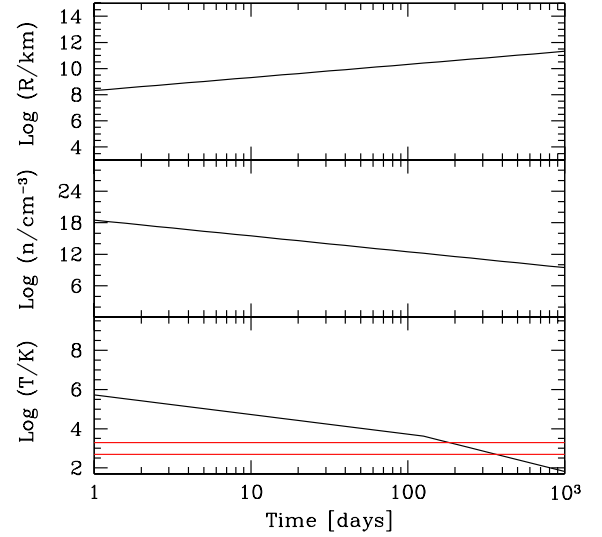


**Figure 2.** Dynamics and thermodynamics of the ejecta for a 195  $M_{\odot}$  PISN. The top, middle and bottom panels show the time evolution of the radius,  $\log R$  (km), number density,  $\log n$  ( $cm^{-3}$ ), and temperature,  $\log T$  (K), of the expanding gas. The temperatures corresponding to the onset of grain condensation ( $T \leq 2000$  K) and to the final state followed by the model ( $T = 500$  K) are indicated with two horizontal lines.

of the initial progenitor mass, but an Fe mass which varies greatly with the mass of the progenitor, being almost negligible for initial stellar masses  $< 200 M_{\odot}$ . It is important to stress that this should be interpreted as the iron mass only after all unstable isotopes have decayed. Indeed, unlike SNI progenitors, PISN progenitors do not build up an iron core before the explosion and the final Fe mass is generated through the decay of  $^{56}\text{Co}$ . We will consider this process in detail as this decay provides the relevant destruction process of CO molecules.

The internal structure of the star at this maximum central density appears to have an approximately constant density,  $\rho_c$ , and temperature,  $T_c$ , up to the outer edge of the helium core (Fryer et al. 2001). We can adopt these values as the initial density and temperature of the volume where the metals are uniformly mixed at shock generation. Indeed, the time that it takes the shocks to propagate through the low-density hydrogen envelope and reach the surface of the progenitor, starting the stellar expansion, is negligible. Adopting this normalization in equation (2), we can follow the evolution of the SN ejecta. The results are shown in Fig. 2. In the top and middle panels we show the evolution of radius and number density of the ejecta of a 195- $M_{\odot}$  PISN as a function of the time elapsed from the explosion. In the bottom panel, we show the corresponding evolution of the temperature. Two different regimes can be identified: in the initial phase of the evolution, the ejecta is radiation-dominated and we assume an adiabatic index  $\gamma = 4/3$ . This appears to be consistent with the internal structure of the 250  $M_{\odot}$  star at maximum central density in the simulation of Fryer et al. (2001), which shows a density and temperature profile in the outer H-envelope compatible with  $\gamma \simeq 4/3$ . However, for  $t > 111.26$  d (where 111.26 d is the  $^{56}\text{Co}$  e-folding time), energy deposition from decaying radioactive elements is negligible and the gas cools adiabatically with  $\gamma = 5/3$ . A comparable thermal history is found by Nozawa et al. (2003), solving the radiative transfer equation and taking into account the energy deposition by radioactive elements. For the same PISN progenitor mass, however, their normalization is slightly higher (by a

**Table 1.** Chemical reactions included in dust formation calculations.

| Solid compound            | Chemical reaction   |
|---------------------------|---|
| $\text{Al}_2\text{O}_3$   | $2\text{Al}+3\text{O} \rightarrow \text{Al}_2\text{O}_3$              |
| Fe                        | $\text{Fe}(\text{g}) \rightarrow \text{Fe}(\text{s})$                 |
| $\text{Fe}_3\text{O}_4$   | $3\text{Fe}+4\text{O} \rightarrow \text{Fe}_3\text{O}_4$              |
| $\text{MgSiO}_3$          | $\text{Mg}+\text{SiO}+2\text{O} \rightarrow \text{MgSiO}_3$           |
| $\text{Mg}_2\text{SiO}_4$ | $2\text{Mg}+\text{SiO}+3\text{O} \rightarrow \text{Mg}_2\text{SiO}_4$ |
| $\text{SiO}_2$            | $\text{SiO}+\text{O} \rightarrow \text{SiO}_2$                        |
| AC                        | $\text{C}(\text{g}) \rightarrow \text{C}(\text{s})$                   |

factor of  $\sim 3$ ) because of the different input stellar models (Umeda & Nomoto 2002).

### 3 MODEL RESULTS

In the model of Todini & Ferrara (2001), the formation of dust grains from a gaseous metal-rich medium is described as a two-step process: (i) the formation of ‘critical clusters’ at the corresponding condensation barrier; and (ii) the subsequent growth of these clusters into macroscopic dust grains through mass accretion. A thorough description of the model, which follows the classic theory of nucleation, can be found in the paper of Todini & Ferrara (2001), to which we refer interested readers.

In the present study, we follow the formation of seven solid compounds, namely,  $\text{Al}_2\text{O}_3$  (corundum), iron,  $\text{Fe}_3\text{O}_4$  (magnetite),  $\text{MgSiO}_3$  (enstatite),  $\text{Mg}_2\text{SiO}_4$  (forsterite),  $\text{SiO}_2$  and amorphous carbon (AC) grains. The corresponding chemical reactions are listed in Table 1. Numerical constants can be found in table 1 of Todini & Ferrara (2001) except for  $\text{SiO}_2$ , for which we have adopted the values used by Nozawa et al. (2003).

It is important to note that, as we will see, AC grains can form also if the ejecta composition is richer in oxygen than in carbon ( $\text{O} > \text{C}$ ) as Clayton et al. (1999) have shown. The formation of CO and SiO molecules in SN ejecta can be very important for dust formation, because carbon atoms bound in CO molecules are not available to form AC grains and SiO molecules take part in the reactions that lead to the formation of  $\text{MgSiO}_3$ ,  $\text{Mg}_2\text{SiO}_4$  and  $\text{SiO}_2$  (see Table 1). Thus the process of molecule formation in the expanding ejecta is followed at temperatures  $T \leq 2 \times 10^4$  K together with the  $^{56}\text{Co} \rightarrow ^{56}\text{Fe}$  radioactive decay, as the impact with energetic electrons produced during this decay represents the main destruction process of CO molecules.

The formation of dust grains is followed until the temperature of the ejecta has decreased to about 500 K, because at this stage condensation processes are terminated for all solid compounds.

The time evolution of the dust mass synthesized in different compounds is shown in Fig. 3 for three representative PISN progenitor masses, 149, 195 and  $250 M_\odot$ . Dust grains start to condense when the temperature of the expanding gas has dropped below 2000 K, about 150–200 d after the explosion (see dotted lines). During this time interval, a fraction of the  $^{56}\text{Co}$  initially present in the ejecta has decayed to Fe. Thus, at the onset of grain condensation, some C atoms are bound in CO molecules and others are available to form AC grains. The resulting dust mass is mainly composed of silicates and magnetite grains. AC grains are the first to form, followed by corundum, forsterite, magnetite and ultimately  $\text{SiO}_2$ . This evolutionary sequence simply reflects the different condensation temperatures. The relative abundances of the different grain species depend on the progenitor mass: the  $149 M_\odot$  star ejects less iron ( $^{56}\text{Co}$ ) than higher mass PISNe and thus its final dust composition

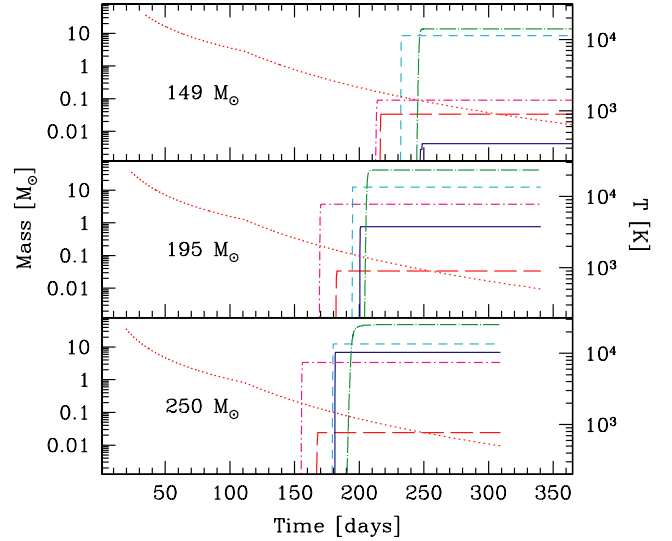


**Figure 3.** Time evolution of the dust mass in different solid compounds synthesized by a  $149 M_\odot$  (top panel),  $195 M_\odot$  (middle panel) and  $250 M_\odot$  (bottom panel) PISN. The different lines correspond to AC (dot-dashed),  $\text{Al}_2\text{O}_3$  (long-dashed),  $\text{Mg}_2\text{SiO}_4$  (dashed),  $\text{Fe}_3\text{O}_4$  (solid) and  $\text{SiO}_2$  (dot-long-dashed). The dotted lines indicate the corresponding values of the temperature of the ejecta.

is characterized by a lower concentration of magnetite and carbon grains (the latter because most of the initial carbon grains are locked in CO molecules).

#### 3.1 Final dust masses

The total dust mass formed in different solid compounds and the total mass of CO molecules synthesized in the ejecta as a function of the progenitor stellar mass are shown in Fig. 4. For all but the

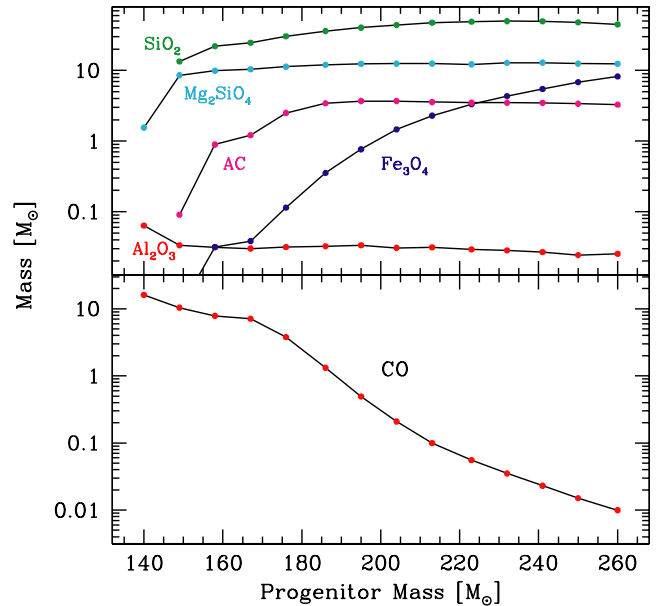


**Figure 4.** Top panel: final dust mass of different solid compounds formed in PISN ejecta as a function of the mass of the stellar progenitors. Bottom panel: total mass of CO molecules synthesized in the ejecta as a function of the initial mass of the stellar progenitors.

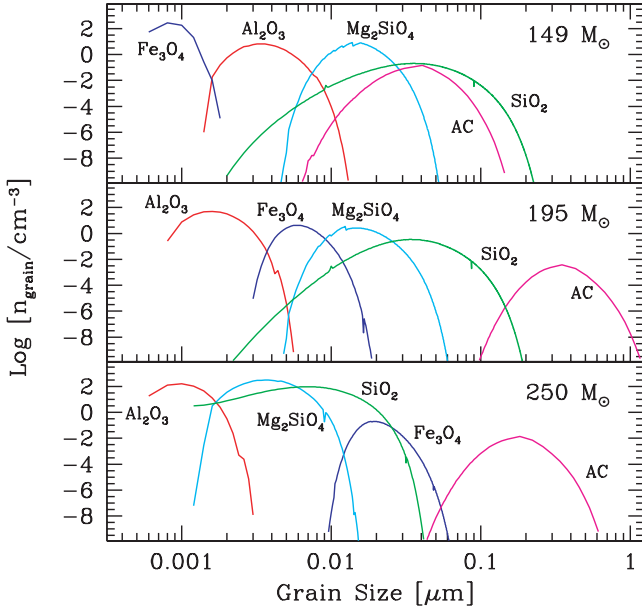


**Figure 5.** Final grain size distributions for different solid compounds synthesized by a  $149 M_{\odot}$  (top panel),  $195 M_{\odot}$  (middle panel) and  $250 M_{\odot}$  (bottom panel) PISN. The distribution is computed when the temperature of the ejecta has decreased to 500 K and formation and accretion are terminated for all compounds.

smallest progenitor star, silicate grains appear to be the dominant dust compounds. Indeed, all SiO molecules initially present in the ejecta take part in the reactions leading to the formation of forsterite and SiO<sub>2</sub> grains, and only CO molecules are left at the end of dust condensation. At the lowest mass bin,  $140 M_{\odot}$ , the initial <sup>56</sup>Co mass is not large enough to favour the formation of magnetite and AC grains, and only Al<sub>2</sub>O<sub>3</sub> and Mg<sub>2</sub>SiO<sub>4</sub> grains are formed. At higher initial stellar masses, the larger <sup>56</sup>Co mass ejected by the PISN favours the formation of carbon and magnetite grains, and the final mass of CO molecules is correspondingly reduced. Note that MgSiO<sub>3</sub> grains are never formed because of the highest condensation temperature and largest nucleation current of Mg<sub>2</sub>SiO<sub>4</sub> grains, which lock all the Mg initially present in the ejecta. Similarly, Fe(s) are never formed because all the Fe that is produced by radioactive decays is locked into magnetite grains. Note that we do not consider the formation of MgO grains which, however, can occur only in the ejecta of the  $140 M_{\odot}$  PISN where Si is less abundant than Mg, and only 40 per cent of the initial Mg mass is depleted on to Mg<sub>2</sub>SiO<sub>4</sub> grains.

### 3.2 Grain size distribution

The final grain size distributions are shown in Fig. 5 for 149, 195 and  $250 M_{\odot}$  PISNe. The characteristic grain sizes range between  $10^{-3}$  and a few  $\times 0.1 \mu\text{m}$ , depending on the grain species and on the mass of the progenitor star. Each dust grain grows by accretion to a final size which depends on the density regime when condensation occurs (higher densities favoring higher accretion rates) and on the abundance of the key species. Indeed, being the first to condense, AC grains tend to have characteristic sizes larger than silicates and magnetite grains. Al<sub>2</sub>O<sub>3</sub> grains are typically small because of the rather low abundance of Al in the ejecta. Larger mass progenitor systems tend to have larger magnetite grains and smaller AC grains. However, the properties of grain size distributions for different pro-

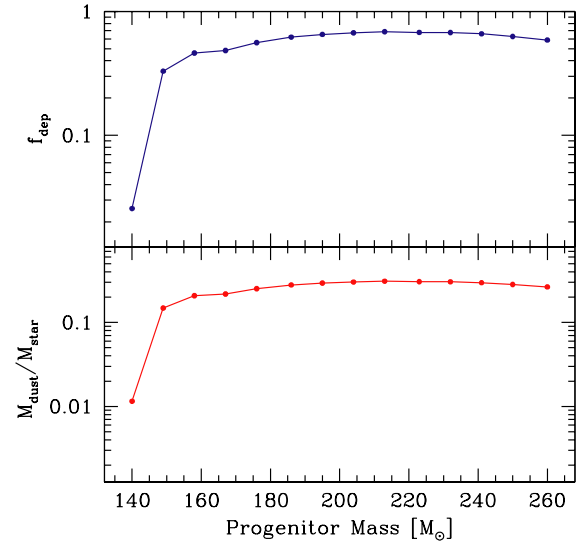


**Figure 6.** Top panel: total dust depletion factor defined as the dust-to-metal mass ratio as a function of the initial progenitor mass. Bottom panel: corresponding values of the ratio between the total dust mass synthesized and the initial progenitor mass.

genitor masses depend on the different thermodynamics of the expanding ejecta which affects the relative amplitude of cooling and nucleation rates. The model predicts that, for all progenitor masses, PISNe lead to the formation of grains with radii smaller than  $1 \mu\text{m}$  but systematically larger than the typical sizes of grains formed in SNIi explosions (Todini & Ferrara 2001), with a reduced scatter among different grain species.

### 3.3 Depletion factors

The cosmological relevance of dust synthesized in PISN explosions will depend mainly on the global properties of dust rather than on the nature and size of different compounds. In Fig. 6 we show the total dust depletion factor, defined as the dust-to-metal mass ratio released in the explosions,  $f_{\text{dep}} = M_{\text{dust}}/M_{\text{met}}$ , as a function of PISN progenitor mass. With the exception of the smallest mass bin,  $f_{\text{dep}}$  ranges between 0.3 and 0.7 and tends to increase with increasing progenitor mass. In the bottom panel of the same figure, we show the ratio of the total dust mass and the initial progenitor stellar mass. For all but the smallest mass bin, the amount of dust formed is between 15 and 30 per cent of the initial stellar mass. The peculiar behaviour of the  $140 M_{\odot}$  progenitor is due to the original elemental composition of its ejecta, which is highly underabundant in Fe and Si, and therefore only corundum and forsterite are synthesized in the final ejecta (see also Fig. 4).

For comparison, in Fig. 7 we show the same quantities but for SNIi. Following Todini & Ferrara (2001), we show two cases corresponding to two different values of the total kinetic energy released in the explosion: case A corresponds to the low kinetic energy model ( $1.2 \times 10^{51}$  erg) and case B refers to the high kinetic energy model ( $1.9 \times 10^{51}$  erg) (see also the original paper of Woosley & Weaver 1995). We also assume two different values for the initial metallicity of the progenitor stars,  $Z = 0$  (dots) and  $Z = Z_{\odot}$  (squares).

The moderate metal yields in SNIi and the effect of fallback of material after the explosion on to the compact remnant lead to depletion factors which are comparable to those of PISNe, with values ranging from 20 per cent up to 70 per cent for  $Z = 0$  progenitors

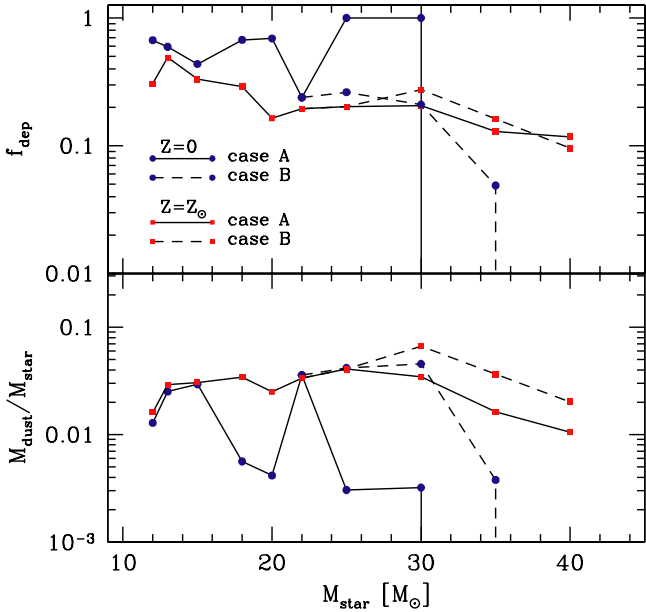


**Figure 7.** As Fig. 6, but for Type II SNe. Cases A and B refer to low ( $1.2 \times 10^{51}$  erg) and high ( $1.9 \times 10^{51}$  erg) kinetic energy scenarios and the dots (squares) represent the dust mass formed from Type II SNe with initial zero (solar) metallicity.

with masses  $<22 M_{\odot}$ . For larger masses, the depletion factor decreases in case B scenarios (higher kinetic energy) because of the larger amount of metals released. For case A scenarios (lower kinetic energy), instead, 25 and  $30 M_{\odot}$  SNeII are predicted to have an  $f_{\text{dep}} = 1$ . This is due to the fact that, because of fallback, these stars eject only a rather small amount of metals, mostly in the form of carbon, which is completely depleted into AC grains. If the stellar progenitors have solar metallicities, the depletion factor ranges between 10 and 50 per cent with a much reduced scatter between cases A and B.

In spite of these large depletion factors, the total mass of dust synthesized by PISNe is significantly higher than that produced by SNeII. Indeed, as already discussed by Todini & Ferrara (2001), in case A scenarios,  $Z = 0$  SNeII synthesize a total dust mass which corresponds to a fraction between 0.3 and 3 per cent of the original stellar progenitor mass (thus  $\sim 0.1$ – $0.6 M_{\odot}$  of dust per SN). These values are slightly larger if case B models are considered. When the initial stellar progenitors have solar metallicities, the resulting dust mass is typically a factor of  $\sim 3$  larger than for the metal-free case but it is always less than 6 per cent of the initial stellar mass.

#### 4 SUMMARY AND DISCUSSION

We have investigated the process of dust formation in the ejecta of first stellar explosions, assuming that the first stars form with characteristic masses of a few hundred  $M_{\odot}$  and explode as PISNe. The study is based on an extension of the model developed by Todini & Ferrara (2001) for SNeII, which accounts for the different initial chemical compositions of the ejecta and dynamical/thermodynamical properties of the ejecta evolution.

The main results of our analysis can be summarized as follows.

(i) During PISN explosions, a significant amount of dust is synthesized out of the heavy elements produced in the progenitor stellar interiors during the main-sequence lifetime and at the onset of the

explosion owing to explosive nucleosynthetic processes. The fraction of the original stellar mass that is converted into dust depends on the progenitor mass, with typical values ranging between 15 and 30 per cent, resulting in  $30$ – $60 M_{\odot}$  of dust produced per SN. These values are much larger than those found for  $Z = 0$  SNeII resulting from stars with masses between 12 and  $40 M_{\odot}$  ( $0.1$ – $0.6 M_{\odot}$ ), even if these stars are assumed to be of solar metallicity ( $0.1$ – $1.8 M_{\odot}$ ).

(ii) Because of the large amount of metals released in PISN explosions, dust depletion factors, defined as the dust-to-metal mass ratio, range between 30 and 70 per cent depending on the progenitor mass.

(iii) The composition of the dust compounds depends critically on the thermodynamics and initial composition of the ejecta, i.e. on the progenitor mass. For the assumed temperature evolution, grain condensation starts 150–200 d after the explosion and silicates, magnetite and AC grains are formed. The dominant compounds for all progenitor masses are  $\text{SiO}_2$  and  $\text{Mg}_2\text{SiO}_4$ , while the contribution of AC and magnetite grains grows with progenitor mass.

(iv) PISN explosions lead to the formation of grains with typical sizes that range between  $10^{-3}$  and a few  $\times 0.1 \mu\text{m}$ ; for all progenitors, grains radii are always smaller than  $1 \mu\text{m}$  but the relative grain size distribution changes depending on the thermodynamics and abundance of the relevant key species. As a general trend, corundum represents the smallest size compound, AC grains tend to form with the largest radii, and silicates and magnetite grains have intermediate sizes.

The above results have been obtained under the assumption that the heavy elements present in the ejecta at the onset of the explosion are uniformly mixed up to the outer edge of the helium core. In previous dust formation models (Kozasa et al. 1989; Todini & Ferrara 2001) this approximation was motivated by the early emergence of X-rays and  $\gamma$ -rays in SN 1987A, which suggested mixing in the ejecta at least up to the helium core edge (Kumagai et al. 1988). The use of multi-dimensional hydrodynamic codes to model the observed light curves has made it clear that mixing occurs on macroscopic scales through the development of Rayleigh–Taylor instabilities: these instabilities arise at the interface between elemental zones and grow non-linearly to produce (i) fingers of heavy elements projected outwards with high velocities, and (ii) mixing of lighter elements down to regions that have lower velocities (Wooden 1997). As a result, the gas in the ejecta is mixed into regions that are still chemically homogeneous and which cool with different time-scales, whereas only small clumps in the ejecta are microscopically mixed. Such a structure affects the process of dust formation, changing both the total amount of dust formed and the relative abundance of different solid compounds, as recently shown by Nozawa et al. (2003).

A related aspect of the model which requires deeper investigation is the assumed temperature structure of the gas within the ejecta. The adopted thermal evolution of the expanding ejecta is motivated by the results of numerical simulations of the internal structure of PISN progenitors (Fryer et al. 2001; Heger & Woosley 2002), and models the impact of the decays of radioactive elements through the change of the adiabatic index from  $\gamma = 4/3$  to  $5/3$  assumed to occur at the  $^{56}\text{Co}$  e-folding time (111.26 d after the explosion). A comparable thermal history is found by Nozawa et al. (2003), solving the radiative transfer equation and taking into account the energy deposition by radioactive elements. For the same PISN progenitor mass, however, their normalization is slightly higher (by a

factor of  $\sim 3$ ) because of the different input stellar models (Umeda & Nomoto 2002).

Finally, to quantify the cosmic relevance of dust formation in the early Universe, we should restrict the analysis to the fraction of the newly formed dust that is able to survive the impact of the reverse shock, following thereafter the fate of the surrounding metal-enriched gas. The process of dust sputtering dissociates the grains into their metal components and might have an important role in cosmic metal enrichment (Bianchi & Ferrara, in preparation). However, new theoretical models seem to indicate that the post-shock temperature enters the regime suitable for dust condensation inside the oxygen layer, because of the high cooling efficiency of this element, but remains substantially higher in the outer He and H layers. If this is the case, then the reverse shock might lead to an increase in the total amount of dust formed rather than decreasing it.

## 5 COSMOLOGICAL IMPLICATIONS

Our analysis shows that if the first stars formed according to a top-heavy initial mass function (IMF) and a fraction of them exploded as PISNe, a large amount of dust was produced in the early Universe. In this section, we discuss some of the main cosmological implications of this result, with particular emphasis on its role in the thermodynamics of the gas that will later be incorporated into subsequent generations of objects.

Recent numerical and semi-analytical models for the collapse of star-forming gas clouds in the early Universe have shown that, because of the absence of metals and the reduced cooling ability of the gas, the formation of low-mass stars is strongly inhibited. In particular, below a critical threshold level of metallicity of  $Z_{\text{cr}} = 10^{-5.5 \pm 1} Z_{\odot}$ , cooling and fragmentation of the gas clouds stop when the temperature reaches a few hundred K (the minimum temperature for H<sub>2</sub> cooling) and the corresponding Jeans mass is of the order of  $10^3$ – $10^4 M_{\odot}$  (Schneider et al. 2002). Gas clouds with mass comparable to the Jeans mass start to gravitationally collapse without further fragmentation, until a central protostellar core is formed which rapidly grows in mass through gas accretion from the surrounding envelope. The absence of metals and dust in the accretion flow and the high gas temperature favour very high accretion efficiencies, and the resulting stars can be as massive as  $600 M_{\odot}$  (Omukai & Palla 2003).

As the gas becomes more and more enriched with heavy elements, the cooling rate increases because of metal (especially C and O) line emission. More importantly, if a fraction of the available metals is depleted on to dust grains, dust–gas thermal exchanges activate a new phase of cooling and fragmentation which enables the formation of gas clumps with low mass (Schneider et al. 2003). In particular, if the metallicity of the star-forming gas clouds exceeds  $10^{-4} Z_{\odot}$ , this dust-driven cooling pathway is irrelevant because cooling via metal-line emission by itself is able to fragment the gas down to characteristic Jeans masses in the range  $10^{-2}$ – $1 M_{\odot}$ . At the same time, if the metallicity of the gas is below  $10^{-6} Z_{\odot}$ , even if all the available metals are assumed to be depleted on to dust grains, the resulting cooling efficiency is too low to activate fragmentation and the resulting Jeans masses are as large as in the metal-free case ( $10^3$ – $10^4 M_{\odot}$ ). Thus we can conclude that the presence of dust is crucial to determine the final mass of stars forming out of gas clouds with metallicities in the critical range  $Z_{\text{cr}} = 10^{-5.5 \pm 1} Z_{\odot}$ . As a reference value, for a metallicity of  $Z = 10^{-5.1} Z_{\odot}$ , if 20 per cent of the metals are depleted on to dust grains ( $f_{\text{dep}} = 0.2$ ) the resulting mass of the collapsing clouds is reduced to  $10^{-2}$ – $10^{-1} M_{\odot}$  and can

lead to low-mass stars. This is fully consistent with the predicted dust mass formed from PISN progenitors (see Fig. 6).

Also, we cannot neglect the fact that our models predict the formation of a significant amount of CO molecules, which can contribute to gas cooling. This aspect needs to be investigated further, although we expect that the presence of CO molecules will be complementary to that of dust in the critical range of metallicities.

Therefore, in the emerging picture of galaxy evolution, the first episodes of star formation were characterized by very massive stars forming according to a top-heavy IMF. It is only when the metals and dust ejected by the first PISNe are able to pollute a substantial fraction of the intergalactic medium (IGM) that an overall transition occurs to a normal IMF forming stars with masses comparable to those that we presently observe in the nearby Universe. The epoch of this transition depends crucially on the process of metal enrichment through the so-called chemical feedback: within metal-enriched regions, if the metallicity lies within the critical range, the presence of dust becomes critical and can no longer be neglected in the thermodynamics of the star-forming gas. It is very likely that the transition will not occur at a single redshift because of the highly inhomogeneous process of metal enrichment (Scannapieco & Ferrara 2003), and that there will be epochs when the two modes of star formation will be coeval in different regions of the Universe.

This in turn might be very important for the reionization history of the IGM. Indeed, very massive metal-free stars are powerful sources of ionizing photons and an early epoch of star formation with a top-heavy IMF can easily match the required high optical depth to electron scattering measured by *WMAP* (Kogut et al. 2003; Spergel et al. 2003; for a general discussion see Ciardi, Ferrara & White 2003). However, an early epoch of reionization is difficult to reconcile with the observed Gunn–Peterson effect in the spectra of  $z > 6$  quasars (Fan et al. 2002), which implies a mass-averaged neutral fraction of  $\sim 1$  per cent. These two observational constraints seem to indicate that the reionization history of the Universe might have been more complex than previously thought, with probably two distinct epochs of reionization separated by a relatively small redshift interval in which the Universe might have recombined again. This intermediate epoch of recombination could be the result of a decrease in the ionizing power of luminous sources, probably due to their metal enrichment and consequent IMF transition.

An early epoch of reionization, as required by *WMAP* data, raises another critical issue: after reionization, the temperature of the IGM starts to decline as a consequence of cosmic expansion. By the time it reaches the observable range of redshifts  $z < 6$  the temperature of the IGM might be too low to match the observed thermal history (Schaye et al. 2000). The presence of a significant amount of dust synthesized by the first very massive SNe might be extremely important to raise the IGM temperature through dust photoelectric heating. To estimate the amount of dust in the IGM required to match the observed thermal history, it is necessary to make specific assumptions about the UV background radiation, the reionization history of the IGM and the grain composition and size distribution (Inoue & Kamaya 2003). Furthermore, the properties of dust grains in the IGM may differ from those directly predicted by dust formation models as a consequence of specific selection rules in the transfer of grains from the host galaxies to the IGM [see Bianchi & Ferrara (in preparation), who find that only grains larger than  $\approx 0.06 \mu\text{m}$  are preferentially ejected in the IGM]. These complications are beyond the scope of the present analysis.

Finally, it is well known that the presence of dust at high redshifts offers an alternative formation channel for molecular hydrogen, the dominant coolant in the early Universe, which, in the absence of

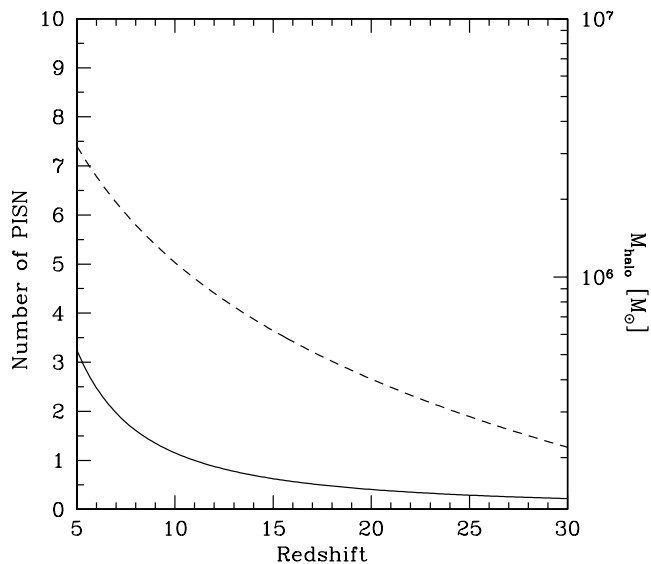


**Figure 8.** The number of PISN required to pollute a host protogalaxy with a dust-to-gas ratio equal to 5 per cent of the Galactic value is shown as a function of redshift (solid line). In the same panel, we show the total mass of the host halo that corresponds to a virial temperature of 1000 K (dashed line).

dust, can form only from the gas phase. In small protogalaxies, the  $H_2$  formation rate on grain surfaces becomes dominant with respect to the formation rate from the gas phase, when the dust-to-gas ratio exceeds roughly 5 per cent of the galactic value (Todini & Ferrara 2001). From this order-of-magnitude estimate, we can derive the number of PISNe required to enrich a small protogalaxy to this level. The results are shown in Fig. 8, where we have assumed the host galaxy to correspond to a halo with a virial temperature of 1000 K and we have considered the dust mass synthesized by a  $195 M_{\odot}$  progenitor (see Fig. 4) as representative of dust formation efficiencies in PISNe. This simple estimate shows that, in the redshift range relevant to these small protogalactic systems ( $z > 10$ –15), one PISN is required to pollute the gas with enough dust that  $H_2$  formation on grain surface starts to be important. This, in turn, might have very important consequences for the star formation activity at high redshift (Hirashita & Ferrara 2002).

## ACKNOWLEDGMENTS

This work was based on the code developed by P. Todini, whose support we gratefully acknowledge. We also thank A. Heger and T. Kozasa for fruitful information and the anonymous referee for valuable suggestions and careful reading of the paper. We acknowledge support from the CNR/JSPP Italy–Japan Seminar Program.

## REFERENCES

Abel T., Bryan G. L., Norman M. L., 2000, *ApJ*, 540, 39  
 Abel T., Bryan G. L., Norman M. L., 2002, *Sci*, 295, 93  
 Bertoldi F., Cox P., 2002, *A&A*, 884, L11  
 Bertoldi F., Carilli C. L., Cox P., Fan X., Strauss M. A., Beelen A., Omont A., Zylka R., 2003, *A&A*, 406, L55  
 Bromm V., Coppi P. S., Larson R. B., 1999, *ApJ*, 527, L5  
 Bromm V., Ferrara A., Coppi P. S., Larson R. B., 2001, *MNRAS*, 328, 969  
 Bromm V., Coppi P. S., Larson R. B., 2002, *ApJ*, 564, 23  
 Carilli C. et al., 2001, *ApJ*, 555, 625  
 Catchpole R. M. et al., 1987, *MNRAS*, 229, 15

Ciardi B., Ferrara A., White S. D. M., 2003, *MNRAS*, 344, L7  
 Cimatti A. et al., 2002, *A&A*, 381, L68  
 Clayton D. D., Liu W., Dalgarno A., 1999, *Sci*, 283, 1290  
 Clayton D. D., Deneault E. A. N., Meyer B. S., 2001, *ApJ*, 562, 480  
 Draine B. T., 2003, *ARA&A*, 41, 241  
 Dunne L., Eales S., Ivison R., Morgan H., Edmunds M., 2003, *Nat*, 424, 285  
 Dwek E., Scalo J. M., 1980, *ApJ*, 239, 193  
 Fan X., Narayanan V. K., Strauss M. A., White R. L., Becker R. H., Pentericci L., Rix H. W., 2002, *AJ*, 123, 1247  
 Fryer C. L., Woosley S. E., Heger A., 2001, *ApJ*, 550, 372  
 Gerardy C. L., Fesen R. A., Höflich P., Wheeler J. C., 2000, *AJ*, 119, 2968  
 Gerardy C. L. et al., 2002, *ApJ*, 575, 1007  
 Granato G. L., Lacey C. G., Silva L., Bressan A., Baugh C. M., Cole S., Frenk C. S., 2000, *ApJ*, 542, 710  
 Heger A., Woosley S. E., 2002, *ApJ*, 567, 532  
 Hernandez X., Ferrara A., 2001, *MNRAS*, 324, 484  
 Hirashita H., Ferrara A., 2002, *MNRAS*, 337, 921  
 Hirashita H., Hunt L. K., Ferrara A., 2002, *MNRAS*, 330, L19  
 Hughes D. M. et al., 1998, *Nat*, 394, 241  
 Inoue A. K., Kamaya H., 2003, *MNRAS*, 341, L7  
 Kogut A. et al., 2003, *ApJS*, 148, 175  
 Kozasa T., Hasegawa H., 1987, *Prog. Theor. Phys.*, 77, 1402  
 Kozasa T., Hasegawa H., Nomoto K., 1989, *ApJ*, 344, 325  
 Kumagai S., Itoh M., Shigeyama T., Nomoto K., Nishimura J., 1988, *A&A*, 197, L7  
 Ledoux C., Bergeron J., Petitjean P., 2002, *A&A*, 385, 802  
 McCray R., 1993, *ARA&A*, 31, 175  
 Morgan H. L., Edmunds M. G., 2003, *MNRAS*, 343, 427  
 Moseley S. H., Dwek E., Giaccum W., Graham J. R., Loewenstein R. F., Silverberg R. F., 1989, *Nat*, 340, 697  
 Nakamura F., Umemura M., 2001, *ApJ*, 548, 19  
 Nakamura F., Umemura M., 2002, *ApJ*, 569, 549  
 Nozawa T., Kozasa T., Umeda H., Maeda K., Nomoto K., 2003, *ApJ*, 598, 785  
 Oh S. P., Nollett K. M., Madau P., Wasserburg G. J., 2001, *ApJ*, 562, L1  
 Omont A., Cox P., Bertoldi F., McMahon R. G., Carilli C., Isaak K. G., 2001, *A&A*, 374, 371  
 Omukai K., Nishi R., 1998, *ApJ*, 508, 141  
 Omukai K., Palla F., 2003, *ApJ*, 589, 677  
 Pettini M., Smith L. J., Hunstead R. W., King D. L., 1994, *ApJ*, 426, 79  
 Pettini M., Kellogg M., Steidel C., Dickinson M., Adelberger K. L., Giavalisco M., 1998, *ApJ*, 508, 539  
 Prochaska J. X., Wolfe A. M., 2002, *ApJ*, 566, 68  
 Ripamonti E., Haardt F., Ferrara A., Colpi M., 2002, *MNRAS*, 334, 401  
 Salvaterra R., Ferrara A., 2003, *MNRAS*, 339, 973  
 Scannapieco E., Schneider R., Ferrara A., 2003, *ApJ*, 589, 35  
 Schaye J., Theuns T., Rauch M., Efstathiou G., Sargent W. L. W., 2000, *MNRAS*, 318, 817  
 Schneider R., Ferrara A., Natarajan P., Omukai K., 2002, *ApJ*, 571, 30  
 Schneider R., Ferrara A., Salvaterra R., Omukai K., Bromm V., 2003, *Nat*, 422, 869  
 Smail I., Ivison R. J., Blain A. W., 1997, *ApJ*, 490, L5  
 Spergel D. L. et al., 2003, *ApJS*, 148, 175  
 Steidel C. C., Adelberger K. L., Giavalisco M., Dickinson M., Pettini M., 1999, *ApJ*, 519, 1  
 Tielens A. G. G. M., 1998, *ApJ*, 499, 267  
 Todini P., Ferrara A., 2001, *MNRAS*, 325, 726  
 Umeda H., Nomoto K., 2002, *ApJ*, 565, 385  
 Whittet D. C. B., 1992, *Dust in the Galactic Environment*, IOP Publishing, Bristol  
 Wooden D. H., 1997, in Bernatowicz T. J., Zinner E. K., eds, *The Astrophysical Implications of the Laboratory Study of Presolar Materials*. Am. Inst. Phys., New York, p. 317  
 Woosley S. E., Weaver T. A., 1995, *ApJS*, 101, 181

This paper has been typeset from a  $\text{\TeX}/\text{\LaTeX}$  file prepared by the author.